# Coexistence in Dipolar Fluids in a Field

Mark J. Stevens and Gary S. Grest

*Corporate Research Science Laboratories, Exxon Research and Engineering Company, Annandale, New Jersey 08801*

We examine two phase coexistence for soft sphere dipolar fluids in an applied field, $H$. Besides being a fundamental test system for theory, dipolar fluids are used as models for ferrofluids. Gibbs ensemble simulations were performed to determine the coexistence curve and an estimate of the critical temperature, $T_c$, and density, $\rho_c$, as a function of applied magnetic field. In zero field we show that coexistence most likely does not occur and if it does can only do so in a narrow range of densities much lower than predicted theoretically. We discuss the structure of soft sphere dipolar systems, which turns out to be much more complex than previously thought.

Fluids of strongly interacting dipoles with a repulsive core potential are the simplest "atomic" fluids in which the interaction is not radially symmetric. Dipolar fluids are models for ferrofluids and their cousins, electrorheological fluids [1–3]. These materials combine the useful properties of magnetic or electric materials and fluids producing various interesting and valuable new properties [4–6]. For hard sphere dipolar fluids there have been several theoretical predictions of a critical point and phase coexistence [1,7–15]. Recent simulations were unable to find the predicted zero field coexistence [16–20]. However, coexistence is known to occur in a field for ferrofluids [21]. Because many applications of these systems are in an applied field, there is much interest in their structure as a function of an applied field. Taking a clue from experiment, we present here results of simulations of dipolar fluids in a field that locate critical points and examine the fluid structure in the vicinity of the critical points.

The original theoretical works on critical points and coexistence in dipolar fluids were based on the van der Waals results for fluctuating dipoles [7,8]. Several recent calculations have also been along this line [11–14]. A different type of coexistence due to magnetic ordering has also been suggested [1,9,14,15]. In this case, coexistence occurs due to the magnetic ordering of the dipoles in the denser phase while the less dense phase is nonmagnetic and isotropic. The magnetic liquid phase has been found in simulations [16,17], but in zero field no coexistence has been observed [18–20].

One of the defining characteristics of dipolar fluids is the presence of chain structures [22]. The particles form chains, because the strong dipolar interaction favors parallel "head-to-tail" alignment. The magnetic liquid phase occurs in part because at high densities the chains become aligned yielding a net magnetism [16]. In ferrofluids, experiments to resolve single particle chains have yet to be done, though evidence exists for long needlelike agglomeration [23]. Simulations offer one means to determine chain structure. In a forthcoming paper we will characterize the dipolar fluid structure as a function of

density, temperature, and applied field. Here, we concentrate on the structure of the two coexisting phases and how it relates to the occurrence of coexistence.

Our simulation model follows that of Wei and Patey [16,17] and Kusalik [24]. We perform Monte Carlo (MC) simulations on soft sphere dipoles with the pair potential

$$
U_{ij}(\mathbf{r}_{ij}) = 4\varepsilon \left(\frac{\sigma}{r_{ij}}\right)^{12}
$$
$$
+ \frac{\mu^2}{r_{ij}^3}\left(\hat{\boldsymbol{\mu}}_i \cdot \hat{\boldsymbol{\mu}}_j - \frac{3}{r_{ij}^2}(\hat{\boldsymbol{\mu}}_i \cdot \hat{\mathbf{r}}_{ij})(\hat{\boldsymbol{\mu}}_j \cdot \hat{\mathbf{r}}_{ij})\right), \quad (1)
$$

where $\sigma$ is the effective particle diameter, $\varepsilon$ is the energy scale, and $\mu_i$ is the dipole moment of the $i$th particle. We will specify variables in reduced form: $T^* = T/\varepsilon$, $\rho^* = \rho\sigma^3$, $\mu^{*2} = \mu^2/\varepsilon\sigma^3$, and $H^* = H\sqrt{\sigma^3/\varepsilon}$. The Ewald sum is used to evaluate the dipole interaction in periodic boundary conditions with the convergence parameter, $\alpha = 5.75$, and reciprocal vectors are summed to $10\pi/L$ where $L$ is the length of the simulation cell. The "tin foil" boundary conditions which allow the magnetically ordered state are used [17]. Canonical constant volume ensemble and Gibbs ensemble simulations have been performed. Below the critical temperature the Gibbs ensemble directly gives the two coexistence densities at a given temperature [25,26]. The number of particles $N$ in the canonical simulations was 256 and in the Gibbs simulations, $N = 512$. Previous simulations [17] found insignificant differences between 256 and 864 particle simulations in zero field. The canonical simulations ran for a least $10^5$ cycles with each cycle comprised of an attempt to translate and rotate each particle. The Gibbs simulations required at least $10^5$ cycles; here, each cycle included an attempt to move each particle once, 100 attempts to change the cell volume, and 500 attempts to exchange particles between the two cells. As has been noted in earlier simulations [18,19] only a small percentage of exchanges is accepted in these Gibbs simulations. Thus, an extremely large number of attempts is needed to gather reasonable statistics. We have verified that both the pressures and the chemical potentials are the same in

the two cells. The pressure is calculated from the virial expression and the chemical potential is calculated from the overlap of the particle insertion and extraction energy distributions [27].

There are three relevant parameters for this problem: the density $\rho$, the dimensionless dipolar coupling strength given by the ratio $\lambda = \mu^2/\sigma^3 T$, and the dimensionless applied field $\eta = \mu H/T$. Strictly speaking $T$ and dipole moment are independent variables, but our soft sphere dipolar potential is sufficiently close to the hard sphere dipolar potential that we can treat them as dependent variables. Thus, while we use $\mu^* = 2.5$, our results can be mapped to other values of $\mu^*$ via $\lambda$. The dimensionless temperature is $\tau = 1/\lambda$.

Our simulations in the Gibbs ensemble were performed with $H^* = 0.25, 0.5, 1.0$, and $2.0$. For all of these fields we found coexistence and list the critical parameters in Table I. For each field only a few points on the coexistence curve were obtained (e.g., see Fig. 1), because the critical temperatures, $\tau_c$, are relatively low, making simulation times prohibitively long. For this reason, $H^* < 0.25$ were not studied. We determined $\tau_c$ by bracketing it between the Gibbs run that gave two clearly distinct densities implying coexistence and the Gibbs run that gave a single peaked density distribution implying that $\tau > \tau_c$. The uncertainty in $\tau_c$, $\pm 0.008$, comes directly from this bracketing. The critical density is taken from the law of rectilinear diameters. With just a few points, estimating the uncertainty in $\rho_c^*$ is difficult, but as $\rho_c$ must be between the two coexisting phase densities, we estimate the uncertainty as $\pm 0.005$.

The plot (Fig. 1) of our calculated $\eta_c$ versus $\tau_c$ exhibits the expected increasing $\tau_c$ with increasing $\eta_c$. Our infinite field $\tau_c$ is $0.18$ which is lower than all predictions for the zero field $\tau_c$. While we are unable to definitively

TABLE I. Critical parameters at various field strengths.

| $H^*$ | $\rho_c^*$ | $\lambda_c$ | $\eta_c$ | $\tau_c$ |
|-------|-----------|-------------|----------|----------|
| 0.25 | 0.032 | 8.93 | 0.65 | 0.112 |
| 0.50 | 0.032 | 6.94 | 1.40 | 0.144 |
| 1.0 | 0.030 | 6.44 | 2.60 | 0.155 |
| 2.0 | 0.035 | 5.95 | 4.75 | 0.168 |

determine the zero field limit of $\tau_c$, an upper bound can be obtained from a spline extrapolation of the data which gives $\tau_c(\eta_c = 0) < 0.07$. This pushes the zero field upper bound of $\tau_c$ to even a lower value than previous simulations [17–20] yielding an even stronger disagreement with analytic calculations.

Our $\rho_c$ (solid circles) are shown in Fig. 2 which also shows experimental data (squares) of Ref. [21]. The critical density is small and independent of applied field, $\rho_c^* = 0.03$. This value represents a lower bound to zero field $\rho_c$. An applied field tends to lower the critical density as the magnetic liquid state occurs at lower densities in higher fields. However, the zero field and infinite field $\rho_c$ are identical in some calculations [11,14].

The experimental data have a regime ($\rho^* \simeq 0.01$) where the critical density varies little with increasing field as in our simulations. At $\rho^* = 0.008$, no coexistence was observed in the experiments up to the maximum attainable field, $\eta = 10.8$. Most of the measured data correspond to a region of small $\eta_c$ variation as $\rho_c$ varies strongly. In these experiments, coexistence only occurs in the presence of a field. Unfortunately, we are unable to examine lower fields to determine if our simulations also cross over to the opposite dependence. The difference between the experimental crossover density and our
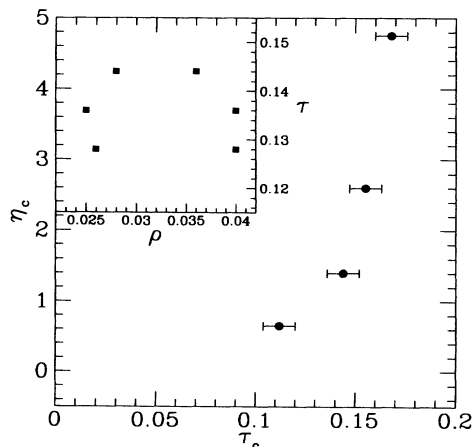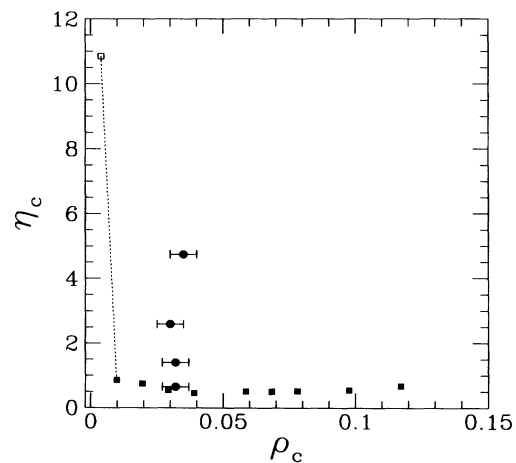


FIG. 1. The dimensionless critical field, $\eta_c$, versus the critical temperature, $\tau_c$. The inset gives the coexistence points calculated for $\eta = 1.40$ ($H^* = 0.5$). There is no coexistence at $\tau \geq 0.15$.



FIG. 2. The critical densities, $\rho_c$, are plotted as a function of the applied field (solid circles). Experimental data from [21] are also given (solid squares). A sharp rise in the critical fields occurs at $\rho < 0.01$, where for the highest field measured ($\eta = 10.8$ and open square) coexistence was not yet observed.

$\rho_c = 0.03$ can be ascribed to the large polydispersity of the experimental system. The average $\lambda$ is 1.0 for the experimental system. However, this yields a much larger critical temperature, $\tau_c = 1.0$, than found in any simulation. Although for a monodisperse system $\tau_c$ should be lower, the discrepancy in the critical temperature is too large to be solely due to polydispersity. Recent experiments [21] show that the solvent plays an important role in determining the critical points. Using a different solvent, coexistence can occur in zero field. As we will show, this implies that the purely repulsive core potential is not a good model for ferrofluids. At least some attractive component is needed.

Our simulations are complementary to recent Gibbs simulations performed by van Leeuwen and Smit [19]. Their core potential included an additional attractive part of the Lennard-Jones (LJ) potential, $-4\varepsilon'(\sigma/r)^6$. Here $\varepsilon'$ is an adjustable parameter that allows variation of the potential from full LJ ($\varepsilon' = \varepsilon$) to the soft sphere potential ($\varepsilon' = 0$) used here. At $\varepsilon' = \varepsilon$ and $\mu^* = 2$, the phase diagram is dominated by the LJ interaction and has a coexistence region (gas-liquid) with a critical point near that of a LJ fluid. As $\varepsilon'$ decreases, the critical density and temperature decrease monotonically until $\varepsilon' = 0.3\varepsilon$ at which $\rho_c^* = 0.10$ and $\tau_c^* = 0.17$. For smaller $\varepsilon'$ they could not find coexistence. Those values are then upper bounds for the zero field critical density and temperature of a soft sphere dipolar system.

The combination of van Leeuwen and Smit's and our results gives lower and upper bounds on $\rho_c$ which allow only a narrow range of densities for coexistence at zero field. Assuming that coexistence occurs at $\varepsilon' = 0$, then a linear extrapolation yields an upper bound $\rho_c^* \approx 0.03$. Since our nonzero field simulations yield about the same value for the lower bound, it appears that for soft (or hard) sphere dipolar systems zero field coexistence is unlikely because the extrapolation is an overestimation.

It is now particularly interesting to determine if the structure of the coexisting phases corresponds to either of the two types of coexistence predicted theoretically. Figure 3 shows projections for the two coexisting densities at $\tau = 0.136$ and $H^* = 1$ with $H$ in the $z$ direction. We find the structure of the two coexisting phases to be similar, in part because the density difference is small. Chains are clearly visible in both phases which are magnetized as expected for such large fields. We definitely do not have a gas-liquid coexistence. Our less dense phase contains chains and cannot be viewed as a gas. In the second theoretical picture, the less dense phase is an isotropic liquid and the dense phase is a magnetic liquid. As $H$ approaches 0, the less dense phase should become isotropic. Our data give no indication of this happening, but we cannot say clearly what happens at very small fields. On the other hand, for $\rho > \rho_c$ the system is predicted to be a magnetic liquid even for $H = 0$. This implies that for $\tau \approx 0.07$, the isotropic-magnetic fluid transition point be near $\rho^* = 0.03$. This in turn would
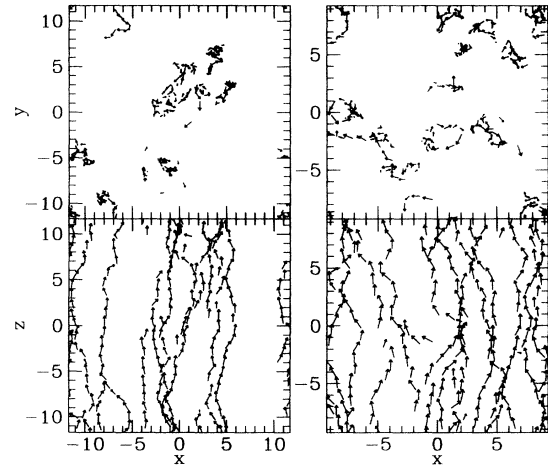
FIG. 3. Projections of dipolar fluids in a magnetic field, $H^* = 1.0$, at $\tau = 0.136$ for $\rho^* = 0.02$ and $\rho^* = 0.04$ which are on the coexistence curves. The field is along the $z$ axis. The arrows give the direction of the dipole moment and the length is scaled with particle radius.

require a very large shift in the density at the transition given that for $\tau = 0.11$, the magnetic transition is at a density close to 0.60 [16,17].

To characterize the system structure we have performed a cluster analysis similar to Weis and Levesque [20]. Since the antiparallel state is precluded by the applied field, we define two particles as bonded if their pair energy is lower than $-0.5\lambda$. This value is at the minimum of the pair energy distribution between peaks due to nearest and next nearest neighbors. Visual examination of run sequences shows that this criterion correctly determines the chains. We have examined the system structure in the vicinity of the critical point. In particular, for $H^* = 1$ we have performed constant volume simulations slightly above ($\tau = 0.176$) and below ($\tau = 0.136$) $\tau_c$ at several densities. We also performed simulations as a function of increasing field at various $\rho$ and $\tau$.

We find that chains are always present even at very low densities. The "bond" energy per $k_B T$ between neighbors is about $-2\lambda$ which for $\tau_c = 0.155$ is 12.88. Thus, it is not surprising even at low densities that chains are present particularly for $\tau < \tau_c$. At $\tau = 0.136$ and $\rho = 0.001$, half of the particles are in chains containing 9 or more particles. At these temperatures, the fluid structure is not "simple" due to the formation of chains.

For $\tau > \tau_c$ and for $\rho \lesssim \rho_c$, the dominant state is the monomer and the distribution of chain size is monotonically decreasing. As $\rho$ or $H$ increases, the longest chains grow at the expense of shorter chains. For example, at $\tau = 0.176$ and $\rho^* = 0.001$, 90% of the chains are monomers and the longest chain in the run is a hexamer. At $\rho^* = \rho_c^*$, the percentage of monomers is reduced to 15% and the largest chain has 41 particles. At this density about 1% of the particles are in chains that percolate

the length of the cell in the field direction. In contrast, at $\tau = 0.136$ long chains dominate the structure near the coexistence densities (cf. Fig. 3). At $\rho^* = 0.02$ which is on the low density coexistence curve, only 2.2% of the particles are monomers. About 40% of the particles are contained in chains of 24–27 particles with the largest chain in the run being 79 particles. In the dense phase, the picture is similar although now the peak in chain size is at about 20 particles and the longest chain is 91 particles. The peak in the chain size corresponds to chain lengths slightly larger than the cell length. Such system size dependence is expected once a chain has percolated the length of the cell, but the picture of chains growing at the expense of shorter chains should be system size independent.

The above results and the solvent dependency of ferrofluid experiments show that the simple purely repulsive core does not model ferrofluids. It would of course be interesting if one can obtain a ferrofluid that is a soft sphere dipolar system, but for present sytems the core potential must have some attractive component to obtain coexistence at $H = 0$ and to shift $\tau_c$ to higher values. Some attractive interaction occurs due to the van der Waals interaction. However, this attraction is at least partly overcome by dispersant molecules necessary to prevent the ferrofluid particles from agglomerating. The solvent dependency implies a solvent mediated attractive interaction which requires some study.

The effect of the attractive part of the core potential can now be easily understood. When $\varepsilon' = \varepsilon$, the system will condense even without the dipole interaction at high $\tau$ ($\tau_c \simeq 0.5$). At these temperatures chaining does not occur because the dipole interaction is too weak and the fluid structure is truly simple. As $\varepsilon'$ decreases lower temperatures are required for condensation, making the dipole interaction relatively stronger. At sufficiently low $\varepsilon'$, the dipole interaction dominates, producing a chained structure. In this regime, the fluid is no longer simple, but reminiscent of a living polymer. Thus, it is not surprising that the various theoretical predictions are poor given that they only treat a simple fluid. It is clear that a simple pair potential like the soft sphere dipole can yield rather complex structures.

Some clue to the structure of coexisting phases in ferrofluids can be obtained from recent experiments on dilute ferroemulsions. The structure of dilute ferroemulsions can be determined by video microscopy ($\rho^* = 0.02$) [28,29]. Within these emulsions are 0.51 $\mu$m oil droplets containing ferrofluid particles. These droplets are superparamagnetic with a dipole moment proportional to the applied field. The microscopy shows that the dense coexisting phase is made of columns with a diameter of several $\sigma$. Thus, the dense coexisting phases are solid, not liquid. The columns exhibit a 2D liquid ordering. The formation of columns in the dilute ferroemulsion further suggests an attractive interaction beyond the dipolar interaction which becomes highly screened between chains. Our simulations show no column formation or liquid ordering of the chains. The chains are flexible implying a repulsive chain-chain interaction (cf. Fig. 3).

[1] A. O. Tsebers, Magnetohydrodynamics **18**, 137 (1982); **19**, 231 (1983).
[2] R. Rosensweig, *Ferrohydrodynamics* (Cambridge University Press, Cambridge, 1985).
[3] J. Popplewell, P. Davies, A. Bradbury, and R. Chantrell, IEEE Trans. Magn. **22**, 1128 (1986).
[4] The Economist **328**, 77 (May 8, 1993); 90 (July 31, 1993).
[5] R. Rosensweig, Sci. Am. **247**, 136 (1982).
[6] T. Halsey and J. Martin, Sci. Am. **269**, 58 (1993).
[7] P. de Gennes and P. Pincus, Phys. Kondens. Materie **11**, 189 (1970).
[8] G. Rushbrooke, G. Stell, and J. Hoye, Mol. Phys. **26**, 199 (1973).
[9] K. Sano and M. Doi, J. Phys. Soc. Jpn. **52**, 2810 (1983).
[10] K. Morozov, A. Pshenichnikov, Y. Raikher, and M. Shliomis, J. Magn. Magn. Mater. **65**, 269 (1987).
[11] Y. A. Buyevich and A. Ivanov, Physica (Amsterdam) **190A**, 276 (1992).
[12] V. I. Kalikmanov, Physica (Amsterdam) **183A**, 25 (1992).
[13] C. Joslin and S. Goldman, Mol. Phys. **79**, 499 (1993).
[14] H. Zhang and M. Widom, Phys. Rev. E **49**, 3591 (1994).
[15] A. Weinstein and S. Safran (unpublished).
[16] D. Wei and G. Patey, Phys. Rev. Lett. **68**, 2043 (1992).
[17] D. Wei and G. Patey, Phys. Rev. A **46**, 7783 (1992).
[18] J.-M. Caillol, J. Chem. Phys. **98**, 9835 (1993).
[19] M. van Leeuwen and B. Smit, Phys. Rev. Lett. **71**, 3991 (1993).
[20] J. Weis and D. Levesque, Phys. Rev. Lett. **71**, 2729 (1993).
[21] R. Rosensweig and J. Popplewell, in *Electromagnetic Forces and Applications* (Elsevier, New York, 1992), p. 83; (private communication).
[22] P. C. Jordan, Mol. Phys. **25**, 961 (1973); **38**, 769 (1979).
[23] D. Krueger, IEEE Trans. Magn. **16**, 251 (1980).
[24] P. Kusalik, J. Chem. Phys. **93**, 3520 (1990).
[25] B. Smit, in *Computer Simulation in Chemical Physics* (Kluwer Academic, Dordrecht, 1993), pp. 173–209.
[26] A. Panagiotopoulos, Mol. Sim. **9**, 1 (1992).
[27] J. Powles, W. Evans, and N. Quirke, Mol. Phys. **46**, 1347 (1982).
[28] J. Bibette, J. Magn. Magn. Mater. **122**, 37 (1993).
[29] J. Liu, E. Lawrence, M. Ivey, G. Flores, and J. Bibette (to be published).